Available online at www.sciencedirect.com
SCIENCE DIRECT
61
JNMU
Journal of Nanjing Medical University, 2008, 22(1):61-65
www.elsevier.com/locate/jnmu
Research Paper

The possible value of ^{18}F-FDG positron emission tomography/computerized tomography imaging in detection of atherosclerotic plaque

Jianwei Yuan[a*], Yanlin Feng[a], Lingxiao Fan[b], Xiaohong He[a]

[a]Department of Nuclear Medicine, Affiliated Foshan Hospital of Sun Yat-sen University, Foshan 528000, Guangdong Province, China;
[b]Office of Scientific Research Management, zhongshan School of Medicine, Sun Yat-sen University, Guangzhou 510080, Guangdong Province, China

Received 13 November 2007

Abstract

Objective:To evaluate the clinical value with positron emission tomography/computerized tomography(PET/CT) imaging for the detection of vulnerable plaque in atherosclerotic lesions. Methods:Sixty people with a age of over 60[mean age (69.2 ± 7.1)years] underwent three dimension(3D) whole-body fluorine-18-2-fluoro-2-deoxy-D-glucose(^{18}F-FDG) PET/CT imaging and were evaluated retrospectively, including 6 cases assessed as normal and 54 cases with active atherosclerotic plaque. Fifty-four cases with SUVs and CT values in the aortic wall of high-FDG-uptake were measured retrospectively. These high-FDG-uptake cases in the aortic wall were divided into three groups according their CT value. Cases in group 1 had high uptake in atherosclerotic lesions of the aortic wall with CT value of less than 60 Hu(soft plaque). Cases in group 2 had high uptake with CT value between 60-100 Hu (intermediate plaque). Cases in group 3 had high uptake with CT value more than 100 Hu(calcified plaque). Group 4 was normal. Results: In group 1, there were 42 high-FDG-uptake sites (average SUV 1.553 ± 0.486). In group 2, there were 30 high-FDG-uptake sites(average SUV 1.393 ± 0.296). In group 3, there were 36 high-FDG-uptake sites(average SUV 1.354 ± 0.189). In group 4, there were 33 normal-FDG-uptake sites (average SUV was 1.102 ± 0.141). The SUVs showed significant difference among the four groups(F = 678.909, P = 0.000). There were also significant difference found between the normal-FDG-uptake group and the high-FDG-uptake groups(P = 0.000, 0.000, 0.001, respectively). Conclusion:Different degrees of 18F-FDG uptake in active large atherosclerotic plaque were shown in different stages of atherosclerotic plaque formation. The soft plaque had the highest FDG uptake in this study. This suggested that 18F-FDG PET/CT imaging may be of great potential value in early diagnosis and monitoring of vulnerable soft plaque in atherosclerotic lesions.

Key words: fluorine-18-2-fluoro-2-deoxy-D-glucose; positron-emission tomography; computerized, tomography; atherosclerosis; vulnerable plaque

INTRODUCTION

Atherosclerosis is one of the leading causes of morbidity and mortality in human beings throughout the world. The rupture of atherosclerotic plaque and thrombi formation are the primary mechanisms of myocardial infarction or a cerebrovascular accident[1]. An atherosclerotic lesion causing an acute cardiovascular event is defined as "vulnerable" plaque. It has been shown that atherosclerotic plaque composition, rather than the degree of arterial stenosis appears to be a critical determinant of atherosclerotic plaque vulnerability and thrombogenicity. The current "gold standard" imaging technique for atherosclerosis is X-ray contrast angiography, which provides a high-resolution definition of the site and severity of luminal stenoses, but no information about plaque composition. It was reported that macrophages contribute extensively to the development

*Corresponding author
E-mail address:yjwei214@hotmail.com

of inflammation in plaque[2-3] and ruptured plaque have large numbers of macrophages[4]. Several pathological studies have clearly demonstrated that macrophages play a key role in both risk of plaque rupture and modulation of the plaque subsequent thrombogenicity[5]. Macrophage density is considered an important determinant of plaque vulnerability. Recently ^{18}F-fluoro-2-deoxy-D-glucose(FDG) positron emission tomography(PET) has been used to image macrophage-rich areas of plaque[6-7]. The objective of this study is to evaluate the clinical value with positron emission tomography/computerized tomography(PET/CT) imaging for the detection of vulnerable plaque in atherosclerotic lesions.

MATERIALS AND METHODS

Sixty people over 60[mean age(69.2 ± 7.1)years] underwent 3D whole-body ^{18}F-FDG PET/CT, including 6 cases assessed as normal and 54 cases with a high-FDG-uptake according to the presence or absence of high-FDG-uptake in the aortic wall. Fifty-four high-FDG-uptake cases were divided into three groups according to the CT value [8]. Cases in group 1 had a high uptake in the aortic wall with CT value less than 60 Hu(soft plaque). Cases in group 2 had high uptake with CT value between 60 Hu to 100 Hu (intermediate plaque). Cases in group 3 had high uptake with CT value more than 100 Hu(calcified plaque). Group 4 was normal.

PET/CT Scanning

All Sixty participants underwent 3D whole-body ^{18}F-FDG PET/CT imaging for their health examination. The image data acquisition was performed on a GEMINI PET/CT scanner(Philips Medical Systems, Cleveland, USA), which combines an Mx8000 computerized tomography scanner(CT) and an Allegro positron emission tomography scanner(PET) with a 3D whole body scan mode. Each person was told to fast for at least 4 h before the intravenous administration of FDG, and their blood glucose level was controlled within the range of 780-1 220 mg/L. The PET/CT scan was began at 60 min after intravenous administration of 5.18 MBq/kg FDG. The parameters for the CT scan were as follows:120 kV, 200 mA, pitch1.00, 0.75 s per ring, and the table increment was 5 mm/s, and 3 min per bed position was used for the emission data acquisition. Emission data was acquired for 8-10 bed positions. The typical scan direction was from the mid thigh to the base of the skull. The data acquisition of the PET scan was started automatically after the CT scan. All people were told to breathe smoothly with their arms up over their head, during the PET and CT data acquisition. The concurrent reconstruction style with the 3D Ramala algorithm was used for the PET image reconstruction, and the CT map was used for the PET data attenuation correction of the same people.

Imaging Analysis

The SUVs in the focal high FDG uptake areas of the aortic wall were detected based on the computerized automatically combined PET/CT imaging results(three highest FDG uptake were measured at random and the medium one was taken). The CT values were demonstrated automatically in the fusion PET/CT imaging. In the normal group, the radioactivity was well-distributed, a non-abnormally high FDG uptake and non-calcified area in the aortic wall was treated as the detective sites, and the SUVs were detected (three sites in the aortic wall were measured at random, the medium one was taken). The aorta segments(arch, ascending, thoracic) were included in detection.

Statistics

Data was expressed as mean±*s*. The statistical software package for social science(SPSS) version 11.0 for windows was used for all data statistical analyses. The relationship among the different groups was determined using the one-way ANOVA method. The relationship between the atherosclerotic plaque groups and normal one was also determined using the LSD method. A *P* value <0.05 was considered statistically significant.

RESULTS

The results of the sixty patients were grouped as per the materials and methods section, and the data from the group sets were retrospectively analyzed.

In group 1, there were 42 high-FDG-uptake sites, with an average SUV of 1.553 ± 0.486(Fig 1). In group 2, there were 30 high-FDG-uptake sites (average SUV 1.393 ± 0.296). In group 3(Fig 2) there were 36 high-FDG-uptake sites,(average SUV 1.354 ± 0.180). In group 4(Fig 3) there were 33 normal-FDG-uptake sites (average SUV 1.102 ± 1.141). The average standard uptake value in group 1 was the highest(Fig 4). Significant differences were found in the SUVs among the four groups(F = 678.909, P = 0.000). There were significant differences between the normal-FDG-uptake group and the high-FDG-uptake groups(P = 0.000, 0.000, 0.001, respectively; Tab 1).

DISCUSSION

Atherosclerotic plaque is characterized by the accumulation of lipids, inflammatory cells and connective tissue within the arterial wall. The mature atherosclerotic plaque consists of a central lipid core and a fibrous cap containing vascular smooth muscle cells and connective tissue, mainly collagen[1]. There is a continuous remodeling process within the plaque, leading to a dynamic balance between erosion and rupture of the fibrous cap(mainly by the macrophages) and repair(by vascular smooth muscle cells). A large number of mac-

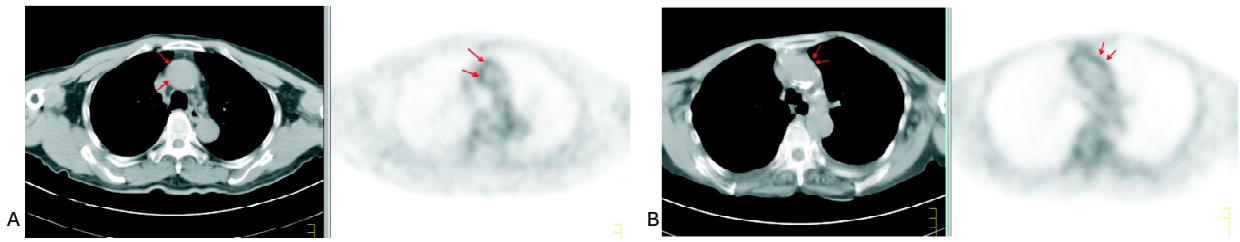

Fig 1 Patterns A and B(soft plaque): PET image in transverse planes show significant high-FDG-uptake in aortic wall(arrows), and the CT image at the same location in transverse planes show no calcified plaque in the aortic wall(CT values between 41 to 56 Hu)

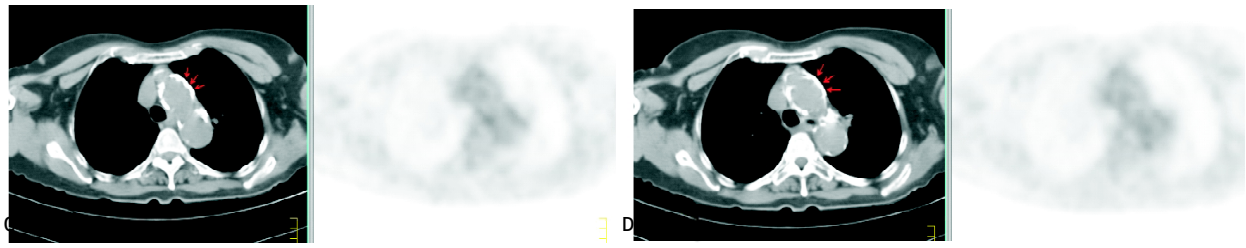

Fig 2 Patterns C and D(calcified plaque): PET/CT image show aortic wall calcification(arrows) and without FDG significant high uptake at the same location

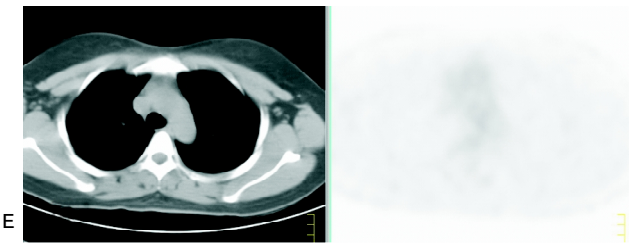

Fig 3 Pattern E(normal group): PET/CT image in transverse plane in the aortic wall show no significant high FDG uptake and no calcified plaque

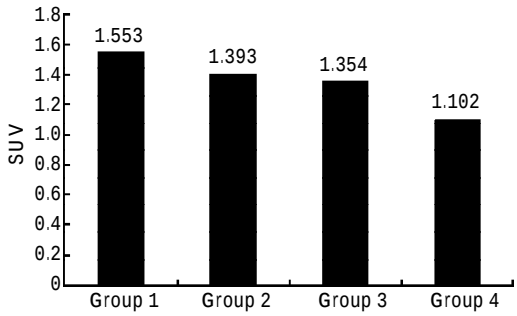

Fig 4 The average standard uptake values of patients in different groups.

Tab 1 SUV of normal-FDG-uptake group compared with high-FDG-uptake groups

	No. of sites	CT value(Hu)	SUV	*P* value
Group 1	42	< 60	1.553 ± 0.486	0.000
Group 2	30	60~100	1.393 ± 0.296	0.000
Group 3	36	> 100	1.354 ± 0.189	0.001
Group 4	33	Normal	1.102 ± 0.141	-

rophages were found in ruptured plaque. Macrophages inhibit collagen formation and are "matrix releasing" degradation proteins, which weaken the fibrous cap and cause rupture. High-risk plaque contain a large lipid core, a thin fibrous cap, many inflammatory cells and few vascular smooth muscle cells[9-10]. By definition, a "vulnerable" plaque can precipitate a clinical event following its rupture, independent of plaque size, but related to the composition of the atheroma[11]. Rupture occur preferentially in plaque containing a soft, lipid-rich core that is covered by a thin cap of fibrous tissue. Compared with intact caps, the ruptured ones usually are thinner, contain less collagen, have fewer smooth muscle cells and are heavily infiltrated by macrophage foam cells[12]. It is therefore clinically important to be able to discriminate between stable and "vulnerable" plaque, for patients' risk stratification and further institution of early therapy.

Different imaging modalities as well as other diagnostic procedures have been developed for the assessment of plaque vulnerability. Angiography is considered to represent the gold standard technique for imaging of the arterial lumen[13]. However, it does not provide information about non-protruding atheromas or plaque composition. Therefore, stable and "vulnerable" plaque cannot be differentiated by means of angiography and plaque rupture cannot be predicted. Intravascular Ultrasound (IVUS) is more sensitive and can identify angiographically invisible plaque and classify them as

soft, fibrous or calcified [14]. But IVUS cannot define its cellular composition, and therefore it cannot diagnose vulnerable plaque. MRI has the potential to identify different stages in plaque formation[15-16], but cannot provide at present data with respect to inflammatory cell activity. ^{18}F-fluoro-2-deoxy-D-glucose (FDG) positron emission tomography(PET) has been used recently to imaging macrophage-rich areas of plaque[6-7]. Recent studies suggest that FDG PET/CT may have an important role in the diagnosing and monitoring of vulnerable plaque[17-18]. In our study, there was a significant difference($P < 0.05$) in ^{18}F-FDG SUV between high-FDG-uptake groups (group1,2,3) and the normal group, which indicated higher ^{18}F-FDG uptake in the atherosclerotic plaque. Among the different kinds of plaque such as soft plaque, intermediate plaque and calcified plaque, we found a significant difference ($F = 678.909$, $P = 0.000$) in SUV existed. The SUV decreased when the CT values of different kinds of plaque increased. The SUV in the soft plaque group was higher than the other two groups (intermediate and calcified plaque). The soft, intermediate and calcified plaque formed in the different atherosclerosis developing stages. The calcified plaque formed when the fibrous cap and atherosclerotic lesion continually deposited, causing the aortic wall harden and become fragile. Different degrees of ^{18}F-FDG uptake in active large atherosclerotic plaque were shown in different stage of atherosclerotic plaque. The soft plaque had the highest FDG uptake in this study. It is suggested that ^{18}F-FDG PET/CT imaging may have great potential value in early diagnosis and monitoring of vulnerable soft plaque in atherosclerotic lesions.

Our research was an initial study on the atherosclerotic plaque based on CT values, and did not divide groups by their pathological significance, so the vulnerable plaque was not equal to the unstable plaque, however the FDG uptake in the atherosclerotic plaque was reflected in the pathological significance to some extent ^{18}(F-FDG is a glucose metabolism image agent). The high glucose metabolic rate in tissues and cells will cause the focal high FDG metabolism. Angitis may have a high FDG metabolism, but it can be differentially diagnosed through the clinical manifestation. Some reports indicated that when the CT map was used for the attenuation correction, a high intensity object such as metal implants, barium in the intestinal tract would revise that correction too much and cause an SUV increment. This deviation has been found to increase as the CT value increased. It is reported by Nakamoto [19] that the deviation of SUV could increase by 45 percent if the CT value indicates 1369 Hu, while perhaps by only a 10 percent increase if the CT value was 200 Hu [20]. In our research, the CT values of calcified plaque were mainly less than 200 Hu, which is a much smaller volume. It needs to be confirmed whether this would produce a significant deviation made by attenuation correction of CT maps.

References

[1] Davies JR, Rudd JH, Weissberg PL. Molecular and metabolic imaging of atherosclerosis. *J Nucl Med* 2004; 45:1898-907.

[2] Robbie L, Libby P. Inflammation and atherothrombosis. *Ann N Y Acad Sci* 2001; 947:167-79.

[3] Libby P. Inflammation in atherosclerosis. *Nature* 2002; 420:868-74.

[4] van der Wal AC, Becker AE, van der Loos CM, Das PK. Site of intimal rupture or erosion of thrombosed coronary atherosclerotic plaque is characterized by an inflammatory process irrespective of the dominant plaque morphology. *Circulation* 1994; 89:36-44.

[5] Corti R, Fuster V, Badimon JJ. Pathogenetic concepts of acute coronary syndromes. *J Am Coll Cardiol* 2003; 41:7S-14S.

[6] Rudd JH, Warburton EA, Fryer TD, Jones HA, Clark JC, Antoun N, et al. Imaging atherosclerotic plaque inflammation with ^{18}F-fluorodeoxyglucose positron emission tomography. *Circulation* 2002; 105:2708-11.

[7] Ogawa M, Ishino S, Mukai T, Asano D, Teramoto N, Watabe H, et al. ^{18}F-FDG accumulation in atherosclerotic plaque: immunohistochemical and PET imaging study. *J Nucl Med* 2004; 45:1245-50.

[8] Schroeder S, Kopp AF, Baumbach A, Meisner C, Kuettner A, Georg C, et al. Noninvasive detection and evaluation of atherosclerotic coronary plaque with multislice computerized tomography. *J Am Coll Cardiol* 2001; 37:1430-35.

[9] Davies JR, Rudd JF, Fryer TD, Weissberg PL. Targeting the vulnerable plaque: the evolving role of nuclear imaging. *J Nucl Cardiol* 2005; 12:234-46.

[10] Ji Hong, Bian Rong-wen, Lou Qing-lin, Zhong Zhao-shu, Zhu Jian-yi, Xie Yu-chun,et al. An analysis of risk factors of carotid atherosclerosis. *Acta Universitatis Medicinalis Nanjing (in chinese)* 2006; 26:769-72.

[11] Virmani R, Kolodgie FD, Burke AP, Farb A, Schwartz SM. Lessons from sudden coronary death: a comprehensive morphological classification scheme for atherosclerotic lesions. *Arterioscler Thromb Vasc Biol* 2000; 20:1262-75.

[12] Falk E, Shah PK, Fuster V: Coronary plaque disruption. *Circulation* 1995; 92:657-71.

[13] Vallabhajosula S, Fuster V. Atheerosclerosis: imaging techniques and the evolving role of nuclear medicine. *J Nucl Med* 1997; 38: 1788-96.

[14] von Birgelen C, Slager CJ, Di Mario C, de Feyter PJ, Serruys PW. Volumetric intracoronary ultrasound: a new maximum confidence approach for the quantitative assessment of progression-regression of atherosclerosis? *Atherosclerosis* 1995; 118(Suppl): S103-13.

[15] Kooi ME, Cappendijk VC, Cleutjens KB, Kessels AG, Kitslaar PJ, Borgers M, et al. Accumulation of ultrasmall superparamagnetic particles of iron oxide in human atherosclerotic plaque can be detected by in vivo magnetic resonance imaging. *Circulation* 2003; 107:2453-8.

[16] Zhao Xi-hai, Cai Zu-long. Advances of MR imaging in coronary atherosclerosis plaque. *Chin J Med Imaing Technol (in chinese)* 2007; 23: 460-2.

[17] Zhang Z, Machac J, Helft G, Worthley S, Tang C, Zaman A, et al. Non-invasive imaging of atherosclerotic plaque macrophage in a

rabbit model with ^{18}F-FDG PET: A histopathological correlation. *BMC Nucl Med* 2006; 6:3.

[18] Ben-Haim S, Israel O. PET/CT for atherosclerotic plaque imaging. *Q J Nucl Med Mol Imaging* 2006; 50:53-60.

[19] Nakamoto Y, Chin BB, Kraitchman DL, Lawler LP, Marshall LT, Wahl RL. Effects of nonionic intravenous contrast agents at PET/CT imaging: phantom and canine studies. *Radiology* 2003; 227: 817-24.

[20] Bujenovic S, Manning F, Chakrabarti R, Ladnier D. Artifactual 2-deoxy-2-[18F]fluoro-D-glucose localization surrounding metallic objects in a PET/CT scanner using CT-based attenuation correction. *Molecular Imaging and Biology* 2003; 5(1): 20-2.

Met as a target in human cancer

George Vande Woude

Van Andel Research Institute, 333 Bostwick NE, Grand Rapids, MI 49506 USA

Inappropriate Met-hepatocyte growth factor/scatter factor (HGF/SF) signaling is a hallmark of most types of solid tumors in humans and often correlates with poor prognosis. There are several mechanisms by which Met signaling is deregulated including Met and/or HGF/SF overexpression, mutation, autocrine signaling, and ligand-independent activation. Because Met is an attractive therapeutic target for a multitude of cancers, extensive research towards finding Met and HGF/SF inhibitors is ongoing.? In parallel with these efforts, several mouse models have been developed in our lab that will be valuable for preclinical testing of Met-targeted therapeutics.

The growth of heterotopic and orthotopic Met-expressing human tumor xenografts in conventional strains of immunocompromised mice inadequately replicates the paracrine stimulation by human HGF/SF (hHGF/SF) that occurs in humans with cancer. To overcome this, our lab generated a mouse strain transgenic for hHGF/SF on a severe combined immunodeficiency (SCID) background. The presence of ectopically expressed hHGF/SF ligand significantly enhances growth of heterotopic subcutaneous xenografts derived from human Met-expressing cancer cells. These results indicate that ectopic hHGF/SF can specifically activate Met in human tumor xenografts and this model provides a powerful tool for evaluating drugs that target Met and/or HGF/SF.

Our lab has also developed a mouse model of the tyrosine kinase ctivating mutations in Met that are observed in hereditary papillary renal carcinomas. Five knockin mouse lines with either wild type or mutant Met were created: wt, D1226N, Y1228C, M1248T, and M1248T/L1193V. Unexpectedly, the different mutant Met lines developed unique tumor profiles including carcinomas, sarcomas, and lymphomas.? These phenotypic differences may result from structural changes that alter the ability of Met to recruit accessory proteins into an active signaling complex ? Understanding the signaling specificity of these mutations is essential to the development of successful therapeutics, especially in light of the different clinical responses to gefitinib or imatinib in patients with different tyrosine kinase mutations in EGFR or c-KIT, respectively. Therefore, our Met mutant mice provide a valuable model for testing the effectiveness of Met inhibitors on tumors containing activating mutations.